# Robust Two-Dimensional Spatial Solitons in Liquid Carbon Disulfide

Edilson L. Falcão-Filho* and Cid B. de Araújo
*Departamento de Física, Universidade Federal de Pernambuco, 50670-901 Recife, Pernambuco, Brazil*

Georges Boudebs,[1] Hervé Leblond,[1] and Vladimir Skarka[1,2]
[1]*LUNAM Université, Université d'Angers, Laboratoire de Photonique d'Angers, EA 4464, 49045 Angers, France*
[2]*Institute of Physics, University of Belgrade, 11000 Belgrade, Serbia*
(Received 29 March 2012; published 2 January 2013; corrected 4 February 2013)

The excitation of near-infrared (2 + 1)D solitons in liquid carbon disulfide is demonstrated due to the simultaneous contribution of the third- and fifth-order susceptibilities. Solitons propagating free from diffraction for more than 10 Rayleigh lengths although damped, were observed to support the proposed soliton behavior. Numerical calculations using a nonlinear Schrödinger-type equation were also performed.

DOI: 10.1103/PhysRevLett.110.013901 PACS numbers: 42.65.Tg, 05.45.Yv, 42.81.Dp

Spatial optical solitons are self-guided beams of light that propagate with invariant shape in nonlinear (NL) media thanks to a balance between diffraction and self-focusing [1–7]. The observation of (1 + 1)-dimensional [(1 + 1)D] spatial solitons was reported in Refs. [8,9]. However, (2 + 1)D optical solitons do not propagate in media with instantaneous cubic nonlinearity (Kerr media) described by the cubic NL Schrödinger (NLS) equation, because catastrophic beam collapse occurs at high powers [10–12]. The stabilization of (2 + 1)D solitons can be achieved due to the saturation of the nonlinearity [13], that can be modeled by means of high-order susceptibilities [14], but intervenes in an effective way in other situations, as a multiple wave interaction, as in the case of quadratic nonlinearities [15], which even allowed prediction [16] and observation of (3 + 1)D spatiotemporal solitons [17].

In quasidiscrete systems such as waveguides arrays, collapse does not occur and (2 + 1)D spatial solitons can be produced [18]; light bullets were predicted [19] and observed [20]. Nonlocality of the nonlinearity is another stabilization process [21]; in air, the noninstantaneous nonlinearity and saturation due to ionization allowed light bullets observation [22]. Also, the photorefractive effect is strongly nonlocal and (2 + 1)D solitons have been observed [23,24]. Thermal effects are also nonlocal and may yield an effective nonlinearity able to stabilize the beam against collapse [25,26]. Spatial solitons were also observed in liquid crystals [27], or can be supported by self-induced transparency [28,29]. Gain-loss balance may also play a role in the formation of "dissipative solitons" [30,31]. More complex patterns, such as optical vortices [32] and their stabilization using a modulation of the linear refractive index [33], were considered. It should also be noted that pure dissipative phenomena (without gain) may lead to beam stabilization against collapse [34,35]; however, although dissipation is unavoidable in real systems, a true steady state cannot be achieved in the absence of gain unless dissipation is negligible. An exception is that of conical or $X$-shaped waves [36,37].

As motivation for the present work we recall that the case of electronic nonlinearities in passive transparent media is of major importance for photonic applications. Only media with ultrafast response may succeed for such applications. Thermal effects are not suited for implementation in practical devices, especially integrated and miniaturized ones involving micrometer or submicrometer sized optics. Moreover the topic is of importance due to many theoretical developments based on the cubic-quintic balance of nonlinearities.

In the frame of the NLS equation with cubic-quintic nonlinearity, in the absence of both gain and dissipation, stability conditions for (2 + 1)D solitons were derived in Ref. [14]. The possibility for detection of stable (2 + 1)D solitons in a homogeneous medium was proposed for an organic crystal, but a clear observation was not reported [38,39]. Here we demonstrate the excitation of (2 + 1)D solitons in liquid $CS_2$ [40] that becomes possible due to the simultaneous contribution of $\chi^{(3)}$ and $\chi^{(5)}$, the third- and fifth-order susceptibility, respectively. Stable self-trapped-damped beams propagating for more than 10 Rayleigh lengths free from diffraction were obtained and characterized.

The third-order refractive index, $n_2 \propto \mathrm{Re}[\chi^{(3)}]$, of $CS_2$ was reported in Ref. [41] while the fifth-order nonlinearity was studied in Refs. [42,43] that provided a value for the fifth-order refractive index, $n_4$. According to Refs. [41,43], $n_2$ and $n_4$ have opposite signs; the three-photon absorption coefficient, $\alpha_4 \propto \mathrm{Im}\chi^{(5)}$, was measured in the present work.

The relation between NL indices and susceptibilities is found by expanding the relation $n = \{1 + \mathrm{Re}[\chi^{(1)} + 3\chi^{(3)}|E|^2 + 10\chi^{(5)}|E|^4]\}^{1/2}$ in a power series of $E$, to obtain $n_2 = 3\mathrm{Re}[\chi^{(3)}]/(4n_0^2\varepsilon_0 c)$ and $n_4 = \frac{1}{(2n_0\varepsilon_0 c)^2} \times$

 

$(\frac{5\mathrm{Re}[\chi^{(5)}]}{n_0} - \frac{9\{\mathrm{Re}[\chi^{(3)}]\}^2}{8n_0^3})$. On the other hand, calculations for the anharmonic oscillator with eigenfrequency $\omega_0$ show that $\chi^{(5)}(\omega;\omega,\omega,\omega,-\omega,-\omega)$ presents a resonance at $3\omega = \omega_0$ in addition to the fundamental resonance at $\omega = \omega_0$, while $\chi^{(3)}(\omega;\omega,\omega,-\omega)$ only presents the latter.

The excitation beam at 920 nm was obtained from an optical parametric amplifier pumped by a Ti:sapphire laser (100 fs, 1 kHz). After passing through a $\lambda/2$ plate and a polarizer the optical parametric amplifier beam passes through a spatial filter, being focused by a lens having 10 cm focal length. The Rayleigh length was 0.1 cm and the beam waist at the focal plane was $16 \pm 2$ $\mu$m.

Figure 1(a) shows the absorbance spectra of $CS_2$ diluted in ethanol. The band centered in $\lambda_0 \approx 317$ nm, identified in Ref. [44], can be excited by the simultaneous absorption of three photons with wavelength at $\lambda = 920$ nm. Note that this absorption band is centered at $\approx \lambda/3$ and thus it is expected that $\chi^{(5)}(\omega;\omega,\omega,\omega,-\omega,-\omega)$ would assume an important role in this case. The value of $n_2 = 3.1 \times 10^{-19}$ m$^2$/W [41] yields $\mathrm{Re}[\chi^{(3)}] = 2.8 \times 10^{-21}$ m$^2$V$^{-2}$. The value of $n_4 = -5.2 \times 10^{-35}$ m$^4$/W$^2$ was adjusted so that the intensity threshold for filamentation obtained numerically coincides with the one observed experimentally. This value of $n_4$ is 2.6 times higher than in Ref. [43], which

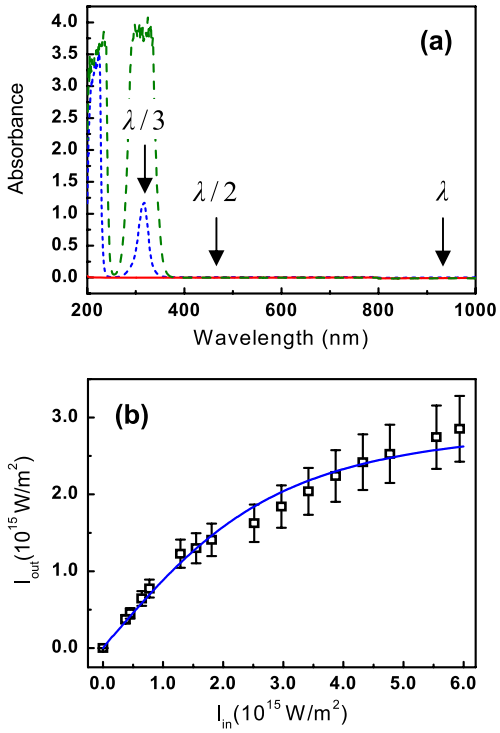


FIG. 1 (color online). (a) Absorbance spectra: solid line designates pure ethanol; dashed (doted) line corresponds to 50 $\mu$l (5 $\mu$l) of $CS_2$ in 2 ml of ethanol. Cell length: 1.0 cm. (b) Transmittance of $CS_2$ versus laser intensity. Cell length: 0.1 cm. The arrows show the wavelengths corresponding to one-, two-, and three-photon absorption.

was obtained at 800 nm, not so close to the third harmonic resonance with the $CS_2$ band at 317 nm. It yields, neglecting the term including $\chi^{(3)}$ in the expression for $n_4$, $\mathrm{Re}[\chi^{(5)}] = -1.2 \times 10^{-39}$ m$^4$ V$^{-4}$, which is 2 orders of magnitude larger than $\{\mathrm{Re}[\chi^{(3)}]\}^2$.

Because of the Kramers-Kronig relations [45–47], such large $\mathrm{Re}[\chi^{(5)}]$ corresponds to a large $\mathrm{Im}[\chi^{(5)}]$, and consequently $\alpha_4$ is not negligible. Therefore the sample transmittance was measured versus the laser intensity to determine $\alpha_4$ using a 0.1 cm long cell. Figure 1(b) shows the output intensity, $I_{\mathrm{out}}$, versus the input intensity, $I_{\mathrm{in}}$. Since the linear absorption and the two-photon absorption coefficients are negligible, we analyzed the results considering the intensity inside the sample described by $dI(z)/dz = -\alpha_4 I^3(z)$. This equation leads to $I_{\mathrm{out}} = I(z = L)$ as a function of $I_{\mathrm{in}}$, where $L = 0.1$ cm is the cell length, and the best fitting provided $\alpha_4 = 5.8 \times 10^{-29}$ m$^3$/W$^2$, taking into account the Fresnel reflection of the cell's faces.

The soliton experiments were carried out using quartz cells either of 1.0 cm or 2.0 cm located in two positions. In one case the entrance face of the cell was located in the focal point (position $A$) to guarantee that the input beam can be described as a plane wave. In the other position the entrance face of the cell was 1.4 mm beyond the focus (position $B$). After the cell a telescope with magnification of 2.9 was used to exploit a large area of the CCD camera used. The camera was in a translation stage with two lenses and a filter in front of it to obtain images at different positions along the beam pathway. The spectra were measured using a spectrometer with resolution of 1.0 nm.

Figure 2 presents beam profile images for different intensities with the cell entrance face either at position $A$ or position $B$. The conditions to observe $(2+1)$D soliton propagation were identified and stable propagation was obtained from $I_{\mathrm{in}} \approx 2.5 \times 10^{11}$ W/cm$^2$ to $3.7 \times 10^{11}$ W/cm$^2$.

From Fig. 2 and from the results for the 2.0-cm-long cell, we conclude that the balance between NL refraction and diffraction results in the generation of $(2+1)$D spatial solitons, which in addition suffer damping due to three-photon absorption. The differences between the results with the 1.0-cm- and 2.0-cm-long cells are mainly due to the $CS_2$ chromatic dispersion.

The output beam spectrum was measured for different input intensities. The line width, $\Delta\omega \approx 62$ nm, measured at $0.4 \times 10^{11}$ W/cm$^2$, increased linearly to $\approx 105$ nm at $\approx 1.1 \times 10^{11}$ W/cm$^2$. From $\approx 1.1 \times 10^{11}$ W/cm$^2$ to $\approx 4.5 \times 10^{11}$ W/cm$^2$ the value of $\Delta\omega$ changes by less than 10%; this is an indication that intensity clamping is occurring. The weak halo around the main beam observed in Figs. 2(e) and 2(j) helps redistribution of the pulse energy. Above $4.5 \times 10^{11}$ W/cm$^2$ further linear growth of $\Delta\omega$ up to $\approx 145$ nm was observed when $I_{\mathrm{in}}$ was increased to $7.5 \times 10^{11}$ W/cm$^2$.

Figure 3(a) presents the output beam waist versus $I_{\mathrm{in}}$ for different cases: when the 1.0 cm cell is at position $A$

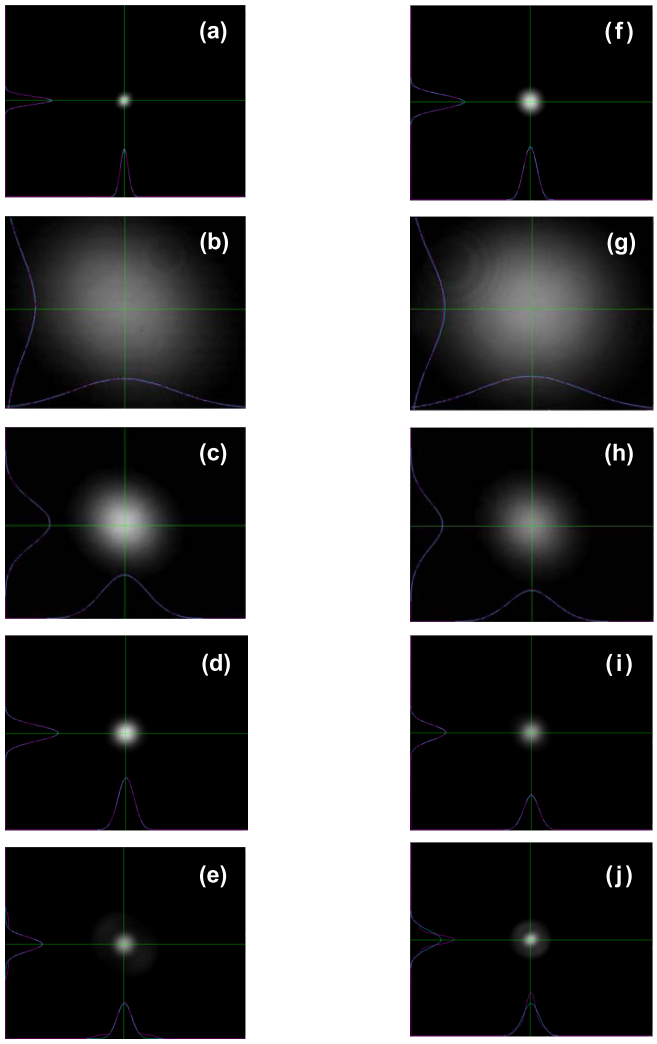


FIG. 2 (color online). Beam images for different laser intensities (cell length: 1.0 cm). (a–e) Data obtained when the entrance face of the cell is at the focal point. (a) Beam profile at the entrance face of the cell; (b) profile at the output face of the empty cell; (c–e) profiles after propagation in $CS_2$ for input intensities of (c) $0.7 \times 10^{11}$ W/cm$^2$, (d) $2.5 \times 10^{11}$ W/cm$^2$, (e) $3.8 \times 10^{11}$ W/cm$^2$. (f–j) Data obtained when the entrance face was 1.4 mm beyond the focus. (f) Beam profile at the entrance face of the cell; (g) profile at the output face of the empty cell; (h–i) beam profiles after propagation in $CS_2$ for input intensities of (h) $0.5 \times 10^{11}$ W/cm$^2$, (i) $1.8 \times 10^{11}$ W/cm$^2$, (j) $2.1 \times 10^{11}$ W/cm$^2$.

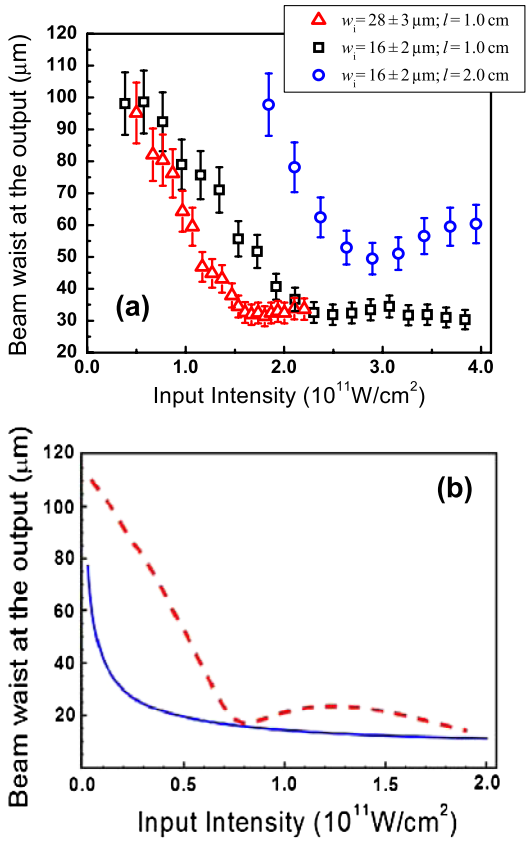


FIG. 3 (color online). (a) Experimental beam waist at the exit face of the cell as a function of the input intensity, for 1.0 cm and 2.0 cm cells positioned at $A$ and $B$. (b) Dashed line: theoretical model considering the cubic and quintic nonlinearities. Solid line: the equilibrium beam waist, as defined in Eq. (4), versus intensity according to the conservative model of Ref. [14].

and $B$ and when a 2.0 cm cell is used in position $A$. Notice that when the 1.0 cm cell is positioned at $A$, for $I_{in} \approx 2.3 \times 10^{11}$ W/cm$^2$ the beam waist becomes $\approx 30$ $\mu$m remaining stable even for higher intensities. Similarly, the output beam waist when the 1.0 cm cell is at position $B$, with input beam waist of $w_i \approx 28$ $\mu$m, exhibits a minimum of about $\approx 30$ $\mu$m at $1.6 \times 10^{11}$ W/cm$^2$ remaining stable for higher intensities. For the 2.0 cm cell, the beam enlarges due to soliton damping, but much less than it would through linear diffraction. At the highest input intensities, the widening becomes more important, since larger nonlinear absorption has reduced the power available at this stage of the propagation. The breathing behavior on the beam waist at high intensities is well reproduced by the theoretical model when the cubic and quintic nonlinearities are taken into account as shown in Fig. 3(b).

In contrast with the stability of the output beam from $2.6 \times 10^{11}$ W/cm$^2$ to $3.7 \times 10^{11}$ W/cm$^2$, the beam profile is distorted above $3.9 \times 10^{11}$ W/cm$^2$ due to a higher NL phase shift that leads to filamentation.

The opposite signs of $n_2$ and $n_4$ provide appropriate conditions for soliton formation in the conservative approximation. The evolution of the optical field $E$ is described by $2ik\frac{\partial E}{\partial z} + \Delta E = -\frac{\omega^2}{c^2}[3\chi^{(3)}E|E|^2 + 10\chi^{(5)}E|E|^4]$, where $\Delta$ is the transverse Laplacian operator and $k$ the light wave number; frequency dispersion is neglected. This is the NLS equation with cubic-quintic nonlinearities. After normalization the equation assumes the form $i\frac{\partial u}{\partial Z} + \frac{1}{2}(\frac{\partial^2 u}{\partial X^2} + \frac{\partial^2 u}{\partial Y^2}) + u|u|^2 - (\nu - i\mu)u|u|^4 = 0$. The notation is the standard one used for the complex Ginzburg-Landau equation;

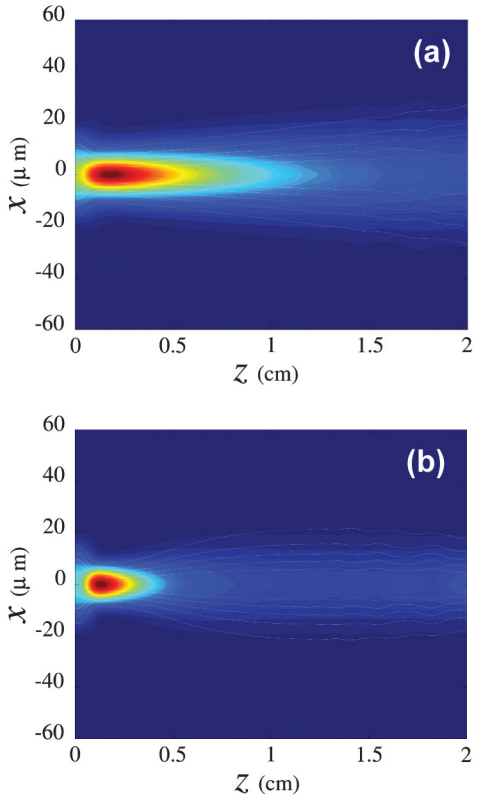


FIG. 4 (color). Evolution of the beam profile during propagation: (a) $I_{\text{in}} = 0.8 \times 10^{11}$ W/cm$^2$; (b) $I_{\text{in}} = 1.6 \times 10^{11}$ W/cm$^2$. The white lines show a contour plot of the normalized intensity $I(z, t)/\max_{t'} I(z, t')$, i.e., the losses due to absorption were removed by normalizing $I$ to 1 at each $z$.

however, dispersion, spectral filtering, linear gain-loss and cubic NL gain-loss coefficients are zero here. $X = x/w_0$, $Y = y/w_0$, and $Z = z/l$, where $w_0$ is the initial beam waist and $l = n_0 \omega w_0^2/c$. The normalized field is $u = E/\sqrt{I_r}$, where the reference intensity is $I_r = 2c^2/3\omega^2 w_0^2 \chi^{(3)}$. The NL coefficients are $\nu - i\mu = -\frac{20}{9} \frac{c^2}{\omega^2 w_0^2} \frac{\chi^{(5)}}{[\chi^{(3)}]^2}$. In the absence of a gain term, the properties of the NLS equation essentially differ from that of the complex Ginzburg-Landau equation. The numerical data yield $\mu = 0.0023$ and $\nu = 0.028$; the propagation distance of 1.0 cm corresponds to $Z = 3.57$.

In the conservative case, i.e., neglecting $\alpha_4$, that corresponds to set $\mu = 0$, it was theoretically proved that stable solitons exist [14]. Moreover, Ref. [14] gives conditions under which a Gaussian input will stabilize to a soliton and express the equilibrium waist as a function of $A$, the initial amplitude of $u$, as $w_e = 2/A\sqrt{1 - 8\nu A^2/9}$ in the normalized units defined above.

Figure 3(b) presents a plot of $w_e$ versus $I_{\text{in}}$ for propagation distance of 1.0 cm. Although there is some discrepancy with the experimental data due to the fact that absorption was neglected, a qualitative agreement between $w_e$ and the measurements is obtained indicating that the phenomenon described in Ref. [14] is observed in the experiment.

The NLS equation was solved by a standard fourth-order Runge-Kutta scheme in $Z$, in the Fourier domain. The NL terms were computed using an inverse and a direct two-dimensional fast-Fourier transform at each substep of the scheme.

Figure 4 shows the evolution of the beam's intensity and profile for two values of $I_{\text{in}}$. Notice that for $I_{\text{in}} = 1.6 \times 10^{11}$ W/cm$^2$, first the beam self-focuses, and then its collapse is arrested by the joint effect of NL absorption and high-order Kerr effect. The beam amplitude decreases after propagation for $Z \approx 0.5$ cm, leading to a regime in which the width of the beam is approximately constant for a long distance.

In summary, due to the simultaneous contributions of $\chi^{(3)}(\omega; \omega, \omega, -\omega)$ and $\chi^{(5)}(\omega; \omega, \omega, \omega, -\omega, -\omega)$, we demonstrated that $CS_2$ may propagate $(2 + 1)$D stable solitons when lasers with proper intensities and wavelengths are employed. A qualitative agreement is found between the theoretical and the experimental results. The small quantitative discrepancy is attributed to the chromatic dispersion that was neglected in the NLS equation, the uncertainties in the intensity measurements, dependence of the $CS_2$ parameters with the pulse duration [48], and deviation of the beam profile from a Gaussian function.

This work was supported by the Brazilian agencies Conselho Nacional de Desenvolvimento Científico e Tecnológico (CNPq) and Fundação de Amparo à Ciência do Estado de Pernambuco (FACEPE). G. B. acknowledges the financial support and hospitality during his visit at the Universidade Federal de Pernambuco. N. B. Aleksic is acknowledged for fruitful discussions. V. S. was supported, in a part, by the Ministry of Science of Serbia under Projects No. OI171006 and No. III 45016.

*Corresponding author.
elff@df.ufpe.br

[1] R. Y. Chiao, E. Garmire, and C. H. Townes, Phys. Rev. Lett. **13**, 479 (1964).
[2] N. N. Akhmediev and A. A. Ankiewicz, *Solitons Nonlinear Pulses and Beams* (Chapman and Hall, London, 1997).
[3] T. Trillo and W. Torruellas, *Spatial Solitons* (Springer, New York, 2001).
[4] B. A. Malomed, D. Mihalache, F. Wise, and L. Torner, J. Opt. B **7**, R53 (2005).
[5] G. I. Stegeman and M. Segev, Science **286**, 1518 (1999).
[6] Y. Kivshar, Nat. Phys. **2**, 729 (2006).
[7] C. Rotschild, B. Alfassi, O. Cohen, and M. Segev, Nat. Phys. **2**, 769 (2006).
[8] A. Barthélémy, S. Maneuf, and C. Froehly, Opt. Commun. **55**, 201 (1985).

[9] J. S. Aitchison, A. M. Weiner, Y. Silberberg, M. K. Oliver, J. L. Jackel, D. E. Leaird, E. M. Vogel, and P. W. E. Smith, Opt. Lett. **15**, 471 (1990).

[10] H. S. Eisenberg, R. Morandotti, Y. Silberberg, S. Bar-Ad, D. Ross, and J. Aitchison, Phys. Rev. Lett. **87**, 043902 (2001).

[11] P. L. Kelley, Phys. Rev. Lett. **15**, 1005 (1965).

[12] L. Bergé, Phys. Rep. **303**, 259 (1998).

[13] N. Akhmediev and J. M. Soto-Crespo, Phys. Rev. A **47**, 1358 (1993).

[14] V. Skarka, V. I. Berezhiani, and R. Miklaszewski, Phys. Rev. E **56**, 1080 (1997).

[15] W. E. Torruellas, Z. Wang, D. Hagan, E. VanStryland, G. Stegeman, L. Torner, and C. Menyuk, Phys. Rev. Lett. **74**, 5036 (1995).

[16] B. A. Malomed, P. Drummond, H. He, A. Berntson, D. Anderson, and M. Lisak, Phys. Rev. E **56**, 4725 (1997).

[17] X. Liu, L. J. Qian, and F. W. Wise, Phys. Rev. Lett. **82**, 4631 (1999).

[18] J. W. Fleischer, M. Segev, N. K. Efremidis, and D. N. Christodoulides, Nature (London) **422**, 147 (2003).

[19] H. Leblond, B. A. Malomed, and D. Mihalache, Phys. Rev. A **83**, 063825 (2011).

[20] S. Minardi *et al.*, Phys. Rev. Lett. **105**, 263901 (2010).

[21] D. Mihalache, D. Mazilu, F. Lederer, B. Malomed, Y. Kartashov, L.-C. Crasovan, and L. Torner, Phys. Rev. E **73**, 025601(R) (2006).

[22] S. Tzortzakis, L. Bergé, A. Couairon, M. Franco, B. Prade, and A. Mysyrowicz, Phys. Rev. Lett. **86**, 5470 (2001).

[23] G. Duree, J. Shultz, G. Salamo, M. Segev, A. Yariv, B. Crosignani, P. Di Porto, E. Sharp, and R. Neurgaonkar, Phys. Rev. Lett. **71**, 533 (1993).

[24] M. Morin, G. Duree, G. Salamo, and M. Segev, Opt. Lett. **20**, 2066 (1995).

[25] C. Rotschild, O. Cohen, O. Manela, M. Segev, and T. Carmon, Phys. Rev. Lett. **95**, 213904 (2005).

[26] Y. Lamhot, A. Barak, O. Peleg, and M. Segev, Phys. Rev. Lett. **105**, 163906 (2010).

[27] M. Peccianti, C. Conti, G. Assanto, A. De Luca, and C. Umeton, Nature (London) **432**, 733 (2004).

[28] M. Blaauboer, B. A. Malomed, and G. Kurizki, Phys. Rev. Lett. **84**, 1906 (2000).

[29] R. El-Ganainy, D. N. Christodoulides, C. Rotschild, and M. Segev, Opt. Express **15**, 10207 (2007).

[30] N. N. Akhmediev and A. Ankiewicz, *Dissipative Solitons: From Optics to Biology and Medicine* (Springer-Verlag, Berlin, 2008).

[31] V. Skarka and N. B. Aleksic, Phys. Rev. Lett. **96**, 013903 (2006).

[32] D. Mihalache, D. Mazilu, F. Lederer, H. Leblond, and B. A. Malomed, Phys. Rev. A **76**, 045803 (2007).

[33] D. Mihalache, D. Mazilu, F. Lederer, H. Leblond, and B. A. Malomed, Phys. Rev. A **81**, 025801 (2010).

[34] G. Fibich, SIAM J. Appl. Math. **61**, 1680 (2001).

[35] T. Passota, C. Sulem, and P. L. Sulem, Physica (Amsterdam) **203D**, 167 (2005).

[36] P. Saari and K. Reivelt, Phys. Rev. Lett. **79**, 4135 (1997).

[37] C. Conti, S. Trillo, P. Di Trapani, G. Valiulis, A. Piskarskas, O. Jedrkiewicz, and J. Trull, Phys. Rev. Lett. **90**, 170406 (2003).

[38] W. Torruelas, B. Lawrence, and G. Stegeman, Electron. Lett. **32**, 2092 (1996).

[39] B. L. Lawrence and G. Stegeman, Opt. Lett. **23**, 591 (1998).

[40] R. L. Sutherland, *Handbook of Nonlinear Optics* (Dekker, New York, 1996).

[41] S. Couris, M. Renard, O. Faucher, B. Lavorel, R. Chaux, E. Koudoumas, and X. Michaut, Chem. Phys. Lett. **369**, 318 (2003).

[42] K. Tominaga and K. Yoshihara, Phys. Rev. Lett. **74**, 3061 (1995).

[43] D. G. Kong, Q. Chang, H. Ye, Y. C. Gao, Y. X. Wang, X. R. Zhang, K. Yang, W. Z. Wu, and Y. L. Song, J. Phys. B **42**, 065401 (2009).

[44] S. P. McGlynn, J. W. Rabalais, J. R. McDonald, and V. M. Scherr, Chem. Rev. **71**, 73 (1971).

[45] V. Lucarini *et al.*, *Kramers-Kronig Relations in Optical Materials Research* (Springer-Verlag, Berlin, 2005).

[46] S. Scandolo and F. Bassani, Phys. Rev. B **51**, 6925 (1995).

[47] S. Scandolo and F. Bassani, Phys. Rev. B **51**, 6928 (1995).

[48] H. Hu *et al.*, *Digest of the 2011 Nonlinear Optics Conference* (Optical Society of America, Washington, 2011) paper NWE12.